COMPARISON OF TWO TECHNIQUES OF ENDOVASCULAR COIL MODELING IN CEREBRAL ANEURYSMS USING CFD

H.G. Morales[⋆†], *I. Larrabide*[†⋆], *M.L. Aguilar*[⋆†], *A.J. Geers*[⋆†], *J.M. Macho*[‡], *L. San Roman*[‡], *and A.F. Frangi*[⋆†§]

[⋆] Center for Computational Imaging & Simulation Technologies in Biomedicine (CISTIB)
Universitat Pompeu Fabra, Barcelona, Spain
[†] Networking Center on Biomedical Research (CIBER-BBN), Barcelona, Spain
[‡] Department of Radiology, Hospital Clinic, Barcelona, Spain
[§] Department of Mechanical Engineering, University of Sheffield, Sheffield, UK.

ABSTRACT

Coiling is the most common endovascular therapy for cerebral aneurysms. In this work, the influence of coil embolization on intra-aneurysmal hemodynamics was studied using two techniques for modeling coils. The first technique represented each coil explicitly and the second one approximated the coil structure with a porous medium. CFD simulations of pre- and post-treatment conditions were compared for one anatomically realistic cerebral aneurysm model. We observed a larger decrease in time- and space-averaged velocity in the aneurysm with the explicit model (92.3%) than with the porous medium model (71.4%). The difference between the two techniques was also demonstrated using virtual contrast injection. Whereas with the explicit model there was a large decrease in the amount of contrast entering the aneurysm and an increase in washout time, these phenomena were not observed with the porous medium model.

Index Terms— Cerebral aneurysm, endovascular coiling, hemodynamics, CFD, virtual treatments.

1. INTRODUCTION

Coiling is the most common endovascular therapy for cerebral aneurysms. It involves the insertion of small biocompatible metal wires inside the aneurysm through a catheter. The goal is to promote the intra-aneurysmal hemodynamic condition that triggers the coagulation cascade to reduce the risk of aneurysm rupture. Such hemodynamic conditions include low velocities and high residence times [1]. However, the intra-aneurysmal hemodynamic alterations induced by endovascular coiling are yet not fully understood.

The research leading to these results has received funding from the European Union Seventh Framework Programme (FP7/2007-2013) under grant agreement nr 223920, VPH-NoE project, has been partially funded by the Industrial and Technological Development Center (CDTI) under the CENIT-cvREMOD program and the Catalonian Department of Innovation, Universities and Enterprise (DIUE), through the EndoTreat project (exp. VALOR2010-00064). Alejandro F. Frangi is partially funded by the ICREA-Academia programme.

To model the effect that coils have on blood flow, several techniques have been developed that can be clustered in two groups. The first one explicitly represents the coils and solves the incompressible Navier-Stokes equations using computational fluid dynamics (CFD) [2][3]. The second group approximates the presence of the devices implicitly with a porous medium, which effectively adjusts the equations used by the CFD solver [4][5].

The purpose of this study is to investigate the influence of endovascular coil on intra-aneurysmal hemodynamics using two coil modeling techniques.

2. MATERIAL

A cerebral aneurysm on a 42-year-old woman was used in this study. The aneurysm was located on the ophthalmic segment of the left internal carotid artery (ICA). The aneurysm had a neck of 6.6 mm and a depth of 7.5 mm, which were measured after a three-dimensional rotational angiography (3DRA) image acquisition. The medical image was obtained with a AXIOM Artis (Siemens Medical Solutions, Erlangen, Germany). The volumetric image consisted of 512x512x442 voxels covering a field of view of 194.75 mm. Aneurysm dimensions and morphology, and patient condition indicated that the case was suitable for endovascular coiling.

3. METHOD

3.1. Image and Surface Mesh Processing

A surface mesh of the aneurysm and parent artery lumen were obtained by segmentation of the medical image. The segmentation was done using a geodesic active region method [6]. After segmentation, small vessels were removed, superficial holes were filled and the final surface of the vasculature was smoothed to simplify the further CFD analysis. Surface mesh edition was done using in-house software, GIMIAS [7].

3.2. Virtual Treatment

The aneurysm geometry was virtually treated using two coil modeling techniques. Both techniques required to isolate the aneurysm from the parent artery by delineating its neck and closing its ostium. The isolated aneurysm had a surface of 199.27 mm^2 and a volume of 280 mm^3. Ten coils with a diameter of 0.254 mm and a total length of 200 cm were inserted. With these coils, a theoretical packing density of 36%, considered the coils as straight cylinders, was obtained. Packing density is defined as the ratio between the volume of the inserted coils and the aneurysm volume and the one imposed is considered to be high in clinical practice using standard coils [8].

3.2.1. Explicit Virtual Coiling

The first coiling technique explicitly represents the endovascular devices. The coils were generated using a dynamic path planning algorithm [9]. Briefly, this coiling technique sequentially places the coils inside the aneurysms until the desired packing density is achieved. Each coil is progressively placed by advancing its tip. Aneurysm perforation, coil collision and migration are not allowed. When the coil tip cannot move further because it is blocked by other coils, it is partially retracted and redirected toward an empty region. The ten coils previously defined were used and a packing density of approximately 33% was achieved.

3.2.2. Implicit Virtual Coiling

The second technique uses a porous medium model to consider the present of the coils inside the aneurysm. This method adapts the Navier-Stokes equations inside the aneurysm by imposing the Darcy porous medium model [10]. In these equations, the porosity of the medium (ε) (the void space through which the fluid flows) and pressure loss S_M due to the motion of the blood flow through the medium are considered. In this model ε=67%.

$$\frac{\partial(\epsilon\rho)}{\partial t} + \nabla(\rho \mathbf{K} U) = 0 \tag{1}$$

$$\frac{\partial}{\partial t}(\varepsilon\rho U) + \nabla(\rho \mathbf{K} U U) = -\varepsilon\nabla p - \nabla(\mathbf{K}\tau) - S_M \tag{2}$$

where ρ is the density of the fluid, t is the time, $\mathbf{K}$ is the porosity tensor, which was assumed isotropic. The term U is the fluid velocity, p is the pressure and τ is the stress tensor. The pressure loss S_M is defined by

$$S_M = \frac{\mu}{k}U + \frac{\rho C_d}{\sqrt{k}}|U|U \tag{3}$$

where, k is the permeability of the porous medium and C_d is drag coefficient factor. In this work, the capillarity theory of Kozeny was used following the CFD study in coiled aneurysms of Kakalis et al.[4]. In the Kozeny theory k is defined by [11]:

$$k = \frac{\varepsilon^3}{cS^2} \tag{4}$$

where $c = 2$ for cylinders and S is the specific surface area (ratio between the coil surface and the aneurysm volume). The coil surface was derived from the ten inserted coils and a value of k=7.204·10^{-5} m^{-2} was obtained. Finally, the term C_d was taken from a Reynolds number-C_d chart [12], under the assumption that the flow is perpendicular to the longitudinal coil axis and that that a coil can be considered as a very thin cylinder (length>>diameter). In our porous medium model, we implemented C_d as a function of local Reynolds number.

3.3. Volumetric Mesh Generation and CFD Modeling

To solve the governing equations of fluid flow in the untreated and coiled models, the fluid domain was discretized using the commercial software ANSYS ICEM CFD v12 (Ansys Inc., Canonsburg, PA). The volumetric meshes for each coiling technique were different since the explicit coils requires small elements around the them to obtain a mesh-independent CFD calculation. As a result, the mesh with the explicit coils was an order of magnitude larger than the mesh with the porous medium (11·10^6 and 0.74·10^6 for the explicit and implicit technique, respectively).

The commercial software ANSYS CFX v12 was used as CFD solver. Blood was considered an incompressible Newtonian fluid with a density of 1066 kg/m^3 and a viscosity of 0.0035 Pa·s. The flow regime was laminar. Vessel and aneurysm surfaces, as well as the coils of the explicit model, had no-slip boundary conditions. A time-dependent physiological flow waveform was imposed at the inlet and pressure waveforms were imposed at the outlets. These in- and outlet conditions were taken from a 1-D model [13].

Three CFD simulations were performed in total, namely untreated, with explicit coils and with porous medium. In each simulation, three cardiac cycles of 0.8 s, discretized in time steps of 0.005 s, were computed and the first one was discarded to remove numerical errors from the initial transient conditions.

At the beginning of the second cycle, the passive transport equation of a massless scalar field was solved following the approach used by Sun et al. [14]. This was done to simulate the injection and propagation of a contrast material through the vasculature. The injection was done during the whole second cycle at a constant value equal to one. The third cardiac cycle was done to visualize the washout phase of the contrast.

Wall shear stress (WSS) at the aneurysm wall, spacial-averaged velocity inside the aneurysm and contrast concentration were calculated during the last two cardiac cycles.

4. RESULTS

Figure 1 depicts the CFD simulations performed at peak systole. Qualitatively, both coiled simulations decrease the intra-aneurysmal velocity as well as the WSS at the aneurysm wall. However, with the porous medium, there is more flow going into the aneurysm as is visualized with the streamlines in figure 1(A).

Figure 2 shows the spatial-averaged intra-aneurysmal velocity and WSS at the aneurysm wall during the third cardiac cycle. The time-averaged velocity values were 0.287 m/s, 0.082 m/s and 0.022 m/s, for the untreated, porous medium and explicit coil model, respectively. The velocity decreases more with the explicit coils (92.3%) than with the porous medium (71.4%). The WSS curves are similar, although there are differences in their distributions (figure 1(C)).

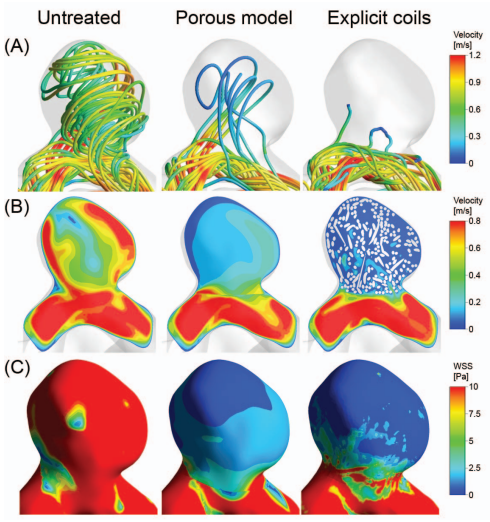


Fig. 1. Hemodynamics variables at peak systole. (A) Instantaneous streamlines color-coded by velocity magnitude. (B) Velocity contour plot on a cut plane in the center of the aneurysm.(C) WSS distribution on the aneurysm wall.

Finally, figure 3 presents the contrast concentration inside the aneurysm along time (figure 3(A)) and for some time points during filling and washout phases (figure 3(B)). For both coiled models, a reduction in the amount of contrast concentration entering the aneurysm is observed, but for the porous medium one, the contrast does not reside as long in the aneurysm as for the explicit model.

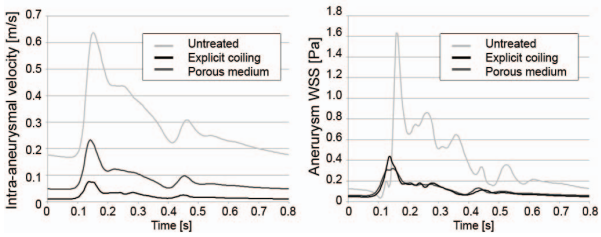


Fig. 2. (A) Average intra-aneurysmal velocity and WSS during one cardiac cycle.

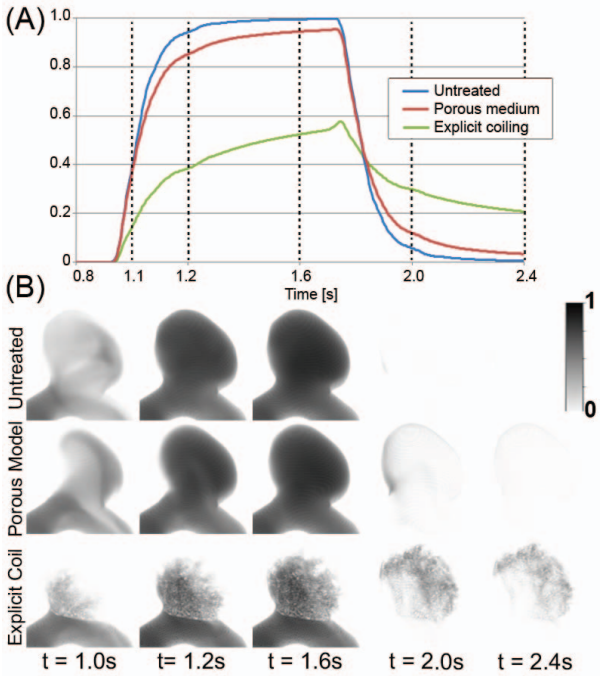


Fig. 3. (A) Contrast concentration inside the aneurysm during two cardiac cycles. (B) Visualization of contrast in some time steps during filling and wash-out phases.

5. DISCUSSION

Both coiled simulations reduced WSS and intra-aneurysmal velocity (figures 1 and 2). Velocity reductions have been reported in a experiment with a phantom coiled aneurysm [15]. Additionally, it has been observed in phantom aneurysms that coils decrease the amount of contrast entering in the aneurysm and increase its residence time [16][17]. These phenomena of the contrast after coiling are only well captured by the explicit coils. This and the simpler Navier-Stokes formulation used in this technique make us believe that it is more reliable than the porous medium and can be consider as our gold standard.

The underestimation of the coiling effect in the porous medium may be due the assumed permeability k. Cha et al. [5] stressed the importance of permeability. Here, k was found with the Kozeny theory following the strategy of a previous work [4]. From equation 3, it is known that with a lower k, the pressure loss S_M will be higher. This leads to lower velocities that should decrease the amount of contrast inside the aneurysm and increase its residence time.

Regarding some features of each coil modeling technique. The porous medium is faster to implement and smaller num-

ber of elements are required, which reduces the computational cost. However, its large disadvantage is the assumed parameters such k. The explicit model, which uses the simpler form of the governing equations of fluid flow, allows us to investigate the effect of coil distribution (heterogeneous for example) and different coil diameters on the hemodynamics.

In future work, the implementation of a more general expression for the permeability [18] can be use such as

$$k = \frac{\varepsilon^3 d_p^2}{a(1-\varepsilon)^2}, \tag{5}$$

where, d_p is the characteristic length of the solid material in the porous medium and a is a constant that parameterizes the microscopic geometry. Both parameters, d_p and a, or the ratio d_p^2/a could be derived from the explicit coil model.

6. CONCLUSION

Two virtual coiling techniques were evaluated for one anatomically realistic cerebral aneurysm using CFD simulations. The explicit coils greatly reduce the intra-aneurysmal velocity, decrease the amount of injected contrast and increase its residence time inside the aneurysm as it has been observed in experiments with phantoms of coiled aneurysms. The porous medium was faster to implement and compute but does not fully catch the effect of decreasing the amount of contrast and increasing its residence time inside the aneurysm.

7. REFERENCES

[1] D M Wootton and D N Ku, "Fluid mechanics of vascular systems, diseases, and thrombosis.," *Annual review of biomedical engineering*, vol. 1, pp. 299–329, 1999.

[2] H G Morales, M Kim, E E Vivas, M-C Villa-Uriol, I Larrabide, T Sola, L Guimaraens, and A F Frangi, "How Do Coil Configuration and Packing Density Influence Intra-Aneurysmal Hemodynamics?," *AJNR. American journal of neuroradiology*, 2011.

[3] J R Cebral and R Löhner, "Efficient simulation of blood flow past complex endovascular devices using an adaptive embedding technique.," *IEEE transactions on medical imaging*, vol. 24, no. 4, pp. 468–76, 2005.

[4] N M P Kakalis, A P Mitsos, J V Byrne, and Y P Ventikos, "The haemodynamics of endovascular aneurysm treatment: a computational modelling approach for estimating the influence of multiple coil deployment.," *IEEE transactions on medical imaging*, vol. 27, no. 6, pp. 814–24, 2008.

[5] K S Cha, E Balaras, B B Lieber, C Sadasivan, and A K Wakhloo, "Modeling the interaction of coils with the local blood flow after coil embolization of intracranial aneurysms.," *Journal of biomechanical engineering*, vol. 129, no. 6, pp. 873–79, 2007.

[6] H Bogunović, J M Pozo, M-C Villa-Uriol, C B L M Majoie, R van den Berg, H A F Gratama van Andel, J M Macho, J Blasco, L San Roman, and A F Frangi, "Automated segmentation of cerebral vasculature with aneurysms in 3DRA and TOF-MRA using geodesic active regions: an evaluation study.," *Medical physics*, vol. 38, no. 1, pp. 210–22, 2011.

[7] I. Larrabide, P. Omedas, Y. Martelli, X. Planes, M. Nieber, J. Moya, C. Butakoff, R. Sebastián, O. Camara, M. De Craene, B. Bijnens, and A. F. Frangi, "GIMIAS: An open source framework for efficient development of research tools and clinical prototypes," in *Functional Imaging and Modeling of the Heart*, 2009, vol. 5528, pp. 417–426, www.gimias.org.

[8] M Sluzewski, W J van Rooij, M J Slob, J O Bescós, C H Slump, and D Wijnalda, "Relation between aneurysm volume, packing, and compaction in 145 cerebral aneurysms treated with coils.," *Radiology*, vol. 231, no. 3, pp. 653–8, 2004.

[9] H G Morales, I Larrabide, M. Kim, M-C Villa-Uriol, J M Macho, J Blasco, L San Roman, and A F Frangi, "Virtual Coiling of Intracranial Aneurysms Based on Dynamic Path Planning," in *Medical Image Computing and Computer Assited Intervention (MICCAI). Toronto, Canada*, 2011, pp. 355–362.

[10] *ANSYS CFX-Solver Theory Guide. Release 12.0*, Canonsburg, PA, 2009.

[11] M Kaviany, *Principles of Heat Transfer in Porous Media*, Springer, New York, 2nd edition, 1995.

[12] Y Nakayama and R F Boucher, *Introduction to Fluid Mechanics*, Arnold, 1998.

[13] P Reymond, F Merenda, F Perren, D A Rüfenacht, and N Stergiopulos, "Validation of a one-dimensional model of the systemic arterial tree.," *American journal of physiology. Heart and circulatory physiology*, vol. 297, no. 1, pp. H208–22, 2009.

[14] Q Sun, A Groth, M Bertram, I Waechter, T Bruijns, R Hermans, and T Aach, "Phantom-based experimental validation of computational fluid dynamics simulations on cerebral aneurysms," *Medical Physics*, vol. 37, no. 9, pp. 5054, 2010.

[15] M H Babiker, L F Gonzalez, F Albuquerque, D Collins, A Elvikis, and D H Frakes, "Quantitative effects of coil packing density on cerebral aneurysm fluid dynamics: an in vitro steady flow study.," *Annals of biomedical engineering*, vol. 38, no. 7, pp. 2293–301, 2010.

[16] S G Imbesi and C W Kerber, "Analysis of slipstream flow in a wide-necked basilar artery aneurysm: evaluation of potential treatment regimens.," *AJNR. American journal of neuroradiology*, vol. 22, no. 4, pp. 721–4, 2001.

[17] S Rudin, Z Wang, I Kyprianou, K R Hoffmann, Y Wu, H Meng, L R Guterman, B Nemes, D R Bednarek, J Dmochowski, and L N Hopkins, "Measurement of flow modification in phantom aneurysm model: comparison of coils and a longitudinally and axially asymmetric stent–initial findings.," *Radiology*, vol. 231, no. 1, pp. 272–6, 2004.

[18] H Chin-Tsau, *"Dynamic Modeling of Convective Heat Transfer in Porous Media," in Handbook of Porous Media*, CRC Press, Boca Raton, 2nd edition, 2005.